Current Research in Food Science 6 (2023) 100497

Contents lists available at ScienceDirect

Current Research in Food Science

journal homepage: www.sciencedirect.com/journal/current-research-in-food-science

Lattice Boltzmann model for freezing of French fries

R.G.M. van der Sman

Wageningen Food & Biobased Research, Wageningen University & Research, the Netherlands

ARTICLE INFO

Handling Editor: Professor A.G. Marangoni

Keywords:
Lattice Boltzmann
Freezing
Simulation
Frying

ABSTRACT

In this paper we present a Lattice Boltzmann model for food freezing, using the enthalpy method. Simulations are performed using the case study of freezing par-fried french fries. The action of par-frying leads to moisture removal from the crust region, which was treated via the initial conditions for the freezing model. Simulations show that under industrial-relevant freezing conditions, the crust region remains either unfrozen or only partially frozen. This result is important for the practical quality problem of dust, which is the phenomenon of fracturing of the crust during finish-frying.

Next to the insight, the Lattice Boltzmann freezing model rendered for the case study of par-fried french fries, we pose that this freezing application is a comprehensive tutorial problem, via which food scientists can be conveniently introduced to the Lattice Boltzmann method. Commonly, the Lattice Boltzmann method has its value in solving complex fluid flow problems, but the complexity of these problems is possibly withholding food scientists to get familiar with the method. Our freezing is solved in 2D, and on a simple square lattice with only 5 particle velocities (a D2Q5 lattice). We hope via this simple tutorial problem, the Lattice Boltzmann method becomes more accessible.

1. Introduction

In this paper, we present a Lattice Boltzmann (LB) scheme for the freezing of par-fried French fries. Freezing of food materials is dominated by heat conduction through the food material, which is mathematically equivalent to diffusion. For the Lattice Boltzmann method, diffusion is a simple process to model, and consequently, we think it is a nice tutorial problem to introduce the method to the food scientist. In a score of publications, we have shown the benefit of the Lattice Boltzmann method for complex fluid flow problems (Van der Graaf et al., 2006)(Kromkamp et al., 2006), but we acknowledge that the complexity of these problems makes it hard for novice users from the food science area, to enter the field. Via addressing the food freezing problem, we think the LB method can be made more accessible.

However, also for the experienced Lattice Boltzmann modeller, this paper is of interest, as it tackles a phase transition problem using the enthalpy method, which is not often used in the LB field, only in rare cases like (Huang et al., 2013; Huo and Rao, 2017). We note that in this study we target the food freezing problem at the length scale of the product, where the resolution of individual ice dendrites is not required. The various Lattice Boltzmann models tackling solidification/melting are recently reviewed (Samanta et al., 2022). Also, recently we have addressed food freezing at the dendrite scale, but that was developed for a different system, a frozen sugar solution, and implemented with the Finite Volume method (van der Sman, 2021). However, the phase field method is also commonly implemented in Lattice Boltzmann (Wang et al., 2019; Samanta et al., 2022).

Phase transitions in food materials are of interest due to the broad temperature range of ice formation, making the material properties like thermal conductivity, specific heat, and enthalpy highly dependent on temperature, cf. (Van der Sman, 2008).

As an example, we take the problem of freezing par-fried French fries. In several research projects, we have been investigating their quality problems arising in their processing at industrial scale (Van der Sman, 2018; van der Sman and van den Oudenhoven, 2023). This problem of simulation of the freezing of (par-fried) french fries is hardly investigated in food science. Studies approaching this problem are (LeBlanc et al., 1990)(Farid, 2002), but they either assumed semi-analytical or empirical models or spherical shapes of products. Recent reviews on food freezing, in general, are by Zhao and Takhar (2017); Fadiji et al. (2021). It is recommended to use the enthalpy method over the apparent specific heat method, which is more accurate in predicting the latent heat release during freezing (Mannapperuma and Singh, 1988, 2001) Scheerlinck et al. (2001) Agnelli et al. (2005) Kiani et al. (2015). This is the approach we will also take in our LB model.

E-mail address: ruud.vandersman@wur.nl.

https://doi.org/10.1016/j.crfs.2023.100497
Received 9 December 2022; Received in revised form 14 March 2023; Accepted 23 March 2023
Available online 8 April 2023

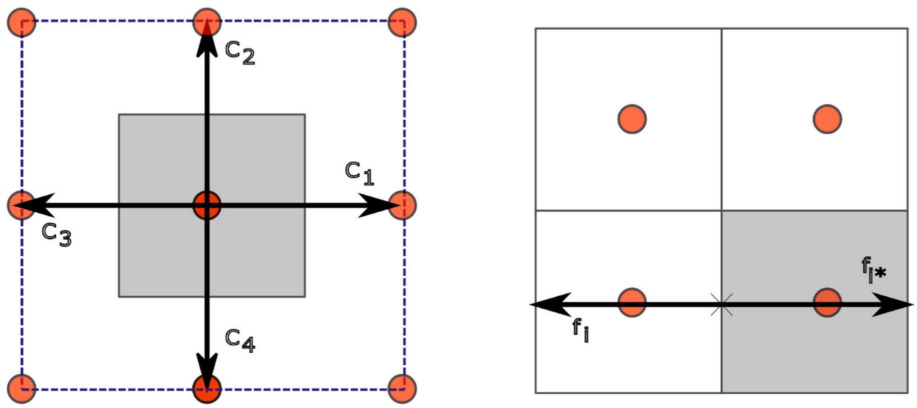

Fig. 1. The D2Q5 lattice used for freezing (left pane), with red dots indicating the lattice sites on a square Bravais lattice, and the arrows indicate the particle velocity set, bringing particles to nearest neighbours. D2Q5 lattice also has rest particles with zero velocity $c_0 = 0$. The grey square indicates the Wigner-Seitz cell. In the right pane, we show a Wigner-Seitz cell at the corner of the computational domain, with particles moving out (f_i) and into (f_{i^*}) the computational domain. Outgoing particles are collected in a ghost layer, surrounding the computational domain, their information is used to determine f_{i^*}, as determined by the boundary condition. (For interpretation of the references to colour in this figure legend, the reader is referred to the Web version of this article.)

In our case of frozen fries, the potato products are subject to par-frying, where they are dipped shortly in a bath with frying oil (Van der Sman, 2018). The purpose of par-frying is to create a crust region with a decreased moisture content and to shorten the final frying process of the frozen product at the point of use (at the consumer's home, or an out-of-home dining facility). In particular, we like to show with this study that this dehydrated crust region does not freeze, during the industrial freezing step. We think this factor is important for the problem of crust fracturing during finish-frying (van der Sman and van den Oudenhoven, 2023), and the occurrence of supercooling, which we will report in a subsequent paper.

2. Model description

The model describes the ice formation in par-fried French fries. The investigated fries have a square cross-section of width $W = 9$ mm. Its length is much larger than the width, and consequently, a 2D model, describing freezing in the cross-section, will suffice. Due to the action of par-frying, the model distinguishes crust and core regions. At the start of the freezing process, the crust region will have a lower moisture content than the core. Furthermore, the crust contains also extra sugars and salt, added in the processing to control colour and taste (van der Sman and van den Oudenhoven, 2023). The thermophysical properties of the food material will be computed based on the composition, and the amount of ice - cf. (Van der Sman, 2008) The model will be implemented with Lattice Boltzmann, based on the enthalpy method. For simplicity's sake, we neglect any volume changes due to ice formation (which has a lower density than liquid water). We first describe the Lattice Boltzmann method, and subsequently, we give the relations for the material properties.

2.1. Lattice Boltzmann model

The Lattice Boltzmann method (LBM) is based on the classical Boltzmann equation, but with space, time, and particle velocity taking discrete values. The LBM describes the evolution of the distribution function of particles residing on a regular (Bravais) lattice, which is often a simple square or cubic lattice. The discrete set of particle velocities $\mathbf{c}_i$ takes the particles on lattice site $\mathbf{x}$ to (next) nearest neighbours at the subsequent time step: $\mathbf{c}_i = \Delta \boldsymbol{x}_i/\Delta t$, with $\Delta \boldsymbol{x}_i$ the vectors connecting lattice site $\mathbf{x}$ to (next) nearest neighbours. This propagation of particles is sketched in Fig. 1.

Following the propagation to neighbouring lattice sites, they collide with other particles arriving at the same lattice site, but from different directions. The collision step is modelled as relaxation towards the equilibrium distribution. For fluid flow, this equilibrium distribution would be the Maxwell-Boltzmann distribution. Often, a single relaxation-time τ is taken for the collision step (Chen and Doolen, 1998). The combined action of collision and propagation on the particle distribution function $f_i(\mathbf{x})$ is described by the following equation:

$$f_i(\mathbf{x}+\mathbf{c}_i\Delta t, t+\Delta t) - f_i(\mathbf{x}, t) = -\omega[f_i(\mathbf{x}, t) - f_i^{eq}(\mathbf{x}, t)] \tag{1}$$

f_i^{eq} is the equilibrium distribution, and $\omega = \Delta t/\tau$. The physics described by the LBM is governed by the conserved quantities, which remain invariant during collisions. Hence, for fluid flow, the collisions need to conserve both mass and momentum. However, for diffusion, the collisions only need to conserve mass (Van der Sman and Ernst, 1999). The mass density ρ is obtained from the zeroth order moment of the distribution function, which remains invariant under collision: $\rho(\mathbf{x}, t) = \sum_i f_i(\mathbf{x},t) = \sum_i f_i^{eq}(\mathbf{x},t)$. In the case of fluid flow, the momentum density is obtained from the first-order moment: $\rho(\mathbf{x}, t)\mathbf{u} = \sum_i \mathbf{c}_i f_i(\mathbf{x}, t) = \sum_i \mathbf{c}_i f_i^{eq}(\mathbf{x},t)$. For the general case, the physics governing LBM is imposed via the moments of the equilibrium distribution. Up to the second order they are denoted as (van der Sman and Van der Graaf, 2008):

$$\begin{aligned} \sum_i f_i^{eq} &= \Phi \\ \sum_i f_i^{eq} c_{i,\alpha} &= \Phi u_\alpha \\ \sum_i f_i^{eq} c_{i,\alpha} c_{i,\beta} &= \Phi u_\alpha u_\beta + \Gamma \mu \delta_{alpha\beta} \end{aligned} \tag{2}$$

with α and β indicating the Cartesian coordinates. $\delta_{\alpha\beta}$ representing the identity matrix, with $\delta_{\alpha\beta} = 1$ if $\alpha = \beta$, and $\delta_{\alpha\beta} = 0$ if $\alpha \neq \beta$. We note, that for this general case, no physical meaning is assigned yet at φ, u_α, μ, and Γ. The partial differential equation, that approximates the action of the LBM, is derived via the mathematical procedure of the Chapman-Enskog expansion (Van Der Sman, 2006). If the LBM only conserves mass (ρ_f), the governing equation becomes (Van Der Sman, 2006; van der Sman and Van der Graaf, 2008):

$$\partial_t \Phi + \partial_\alpha \Phi u_\alpha = \partial_\alpha M \partial_\alpha \mu \tag{3}$$

with the mobility $M = \Gamma(1/\omega - \frac{1}{2})\Delta t$. In the governing equation ∂_α represents component the nabla vector operator ∇. The Einstein convention of summation over double indices is implied. This notation is commonplace in the field of LBM, and thus it is also used here.

The above general scheme has been used for describing the convection-diffusion of a phase field, describing the microstructural development of emulsions (van der Sman and Van der Graaf, 2008). There φ is the order parameter of the phase field, u_α is the velocity field, and μ is the chemical potential. Here, we will use the general expression to design a LB scheme, which simulates freezing following the enthalpy method.

In the enthalpy method, the conserved quantity is energy (density), which should include the latent heat stored in the ice fraction. The energy density e of the freezing fry changes due to heat conduction:

$$\begin{aligned} \partial_t e &= \partial_\alpha j_\alpha \\ j_\alpha &= \lambda_{eff} \partial_\alpha T \end{aligned} \tag{4}$$

j_α is the heat flux due to conduction, with λ_{eff} the thermal conductivity, and T the temperature. The energy density is defined as:

$$e = \rho_{eff} c_{p,eff}(T - T_0) - \varphi_{ice} h_{ice} \tag{5}$$

ρ_{eff} is the mass density of the food material, $c_{p,eff}$ is the specific heat, T_0 is the reference temperature (zero Celsius), φ_{ice} is the volume fraction of ice, and h_{ice} is the latent heat of fusion for ice crystals (given in [J/m^3]). Note that the latent heat contribution to e is negative, meaning that ice formation will generate heat. The material properties λ_{eff}, and $\rho_{eff} c_{p,eff}$ are is dependent on the amount of ice φ_{ice}, as described below.

The above partial differential equation can be modelled by LBM, under the condition of the following moments to the equilibrium particle distribution function:

$$\begin{aligned} \sum_i f_i^{eq} &= e \\ \sum_i f_i^{eq} c_{i,\alpha} &= 0 \\ \sum_i f_i^{eq} c_{i,\alpha} c_{i,\beta} &= \Gamma c^2 (T - T_0)\delta_{\alpha\beta} \end{aligned} \tag{6}$$

For French fries, one can assume that the thermal conductivity is isotropic. Hence, the effective thermal conductivity can be linked to the relaxation parameter and Γ via:

$$\lambda_{eff} = \Gamma c^2 \left(\frac{1}{\omega} - \frac{1}{2}\right)\Delta t \tag{7}$$

The above constraints for the moments of the equilibrium distribution are already satisfied by a so-called D2Q5 lattice (Huang et al., 2013). This type of lattice is already shown in Fig. 1, which is a square lattice with uniform lattice spacing Δx, a rest particle with $\mathbf{c}_0 = 0$ and 4 other particles propagating to nearest neighbours with velocity $|\mathbf{c}_i| = c = \Delta x / \Delta t$.

The explicit expression of the equilibrium function, adhering to the above constraints is:

$$f_i^{eq} = w_i \Gamma c^2 (T - T_0) \tag{8}$$

for $i > 0$, and

$$f_0^{eq} = e - \sum_{i>0} f_i^{eq} \tag{9}$$

For the weight factors hold $w_i = \frac{1}{2}$. The actual temperature needs to be computed using Eq. (5), using the total energy density e.

The computational domain is a quarter of the cross-section. We apply symmetric boundary conditions at x = 0 and y = 0. At $x = \frac{1}{2}W$, and $y = \frac{1}{2}W$ we assume a constant temperature, equal to that of the freezing airflow.

The boundaries of the computational domain coincide with the boundaries of the Wigner-Seitz cells of the Bravais lattice, at which we impose the boundary conditions, as is indicated in Fig. 1. We divide the square computational domain into $N \times N$ lattice cells, implying $\Delta x = \frac{1}{2} H/N$.

The Dirichlet condition on the outer boundary is defined as follows:

$$c(f_i(\mathbf{x}, t) - f_{i*}(\mathbf{x}^*, t)) = j_e = \frac{\lambda_{eff}}{\frac{1}{2}\Delta x}[T(\mathbf{x}) - T_{air}] \tag{10}$$

j_e is the conductive heat flux through the outer boundary, with a normal vector parallel to $\mathbf{c}_i$, and with $\mathbf{c}_{i^*} = -\mathbf{c}_i$. $f_i(\mathbf{x}, t)$ are particles moving out of the computational domain, and $f_{i*}(\mathbf{x}^*, t))$ are particles moving into the computational domain, cf. (Van der Sman, 1997).

The symmetry boundary condition is:

$$f_i(\mathbf{x}, t) - f_{i*}(\mathbf{x}^*, t)) = 0 \tag{11}$$

This can be interpreted as a simple reflection of f_i on the boundary. The magnitude of the timestep Δt is determined by the stability criteria of the diffusion LB scheme:

$$Fo^* = \frac{\alpha_{eff}\Delta t}{\Delta x^2} < \frac{1}{2} \tag{12}$$

Fo^* is the grid Fourier number, and $\alpha_{eff} = \lambda_{eff}/\rho_{eff} c_{p,eff}$ is the thermal diffusivity. Note, that the same stability condition holds for Finite Volume and Finite Difference schemes with Euler forward time integration. If $\omega = 1$ the LBM is mathematically equivalent with these schemes (Van der Sman, 2006).

2.2. Material properties

From the local composition of the unfrozen phase, we compute the water activity and the freezing point. The composition is characterized by the mass fractions of unfrozen water (y_w), starch (y_c), sugars (y_s), and salt (NaCl) (y_a). The core region of the fry is assumed to contain only water and starch.

The water activity is computed using the Flory-Huggins-Free-Volume (FHFV) theory (Van der Sman and Meinders, 2011), augmented with the Pitzer equation accounting for the contribution of the salt (Van der Sman, 2008, 2012). For the FHFV theory, the mass fractions are converted into volume fractions, using known mass densities, cf. (Van der Sman, 2008). The FHFV theory takes the T_g of the starch/water system (Van der Sman, 2008), which is modified due to the presence of salt cf. (Van der Sman and Broeze, 2014).

The relation between water activity a_w and freezing point T_f is (Van der Sman and Meinders, 2011):

$$\ln(a_w) = \left(\frac{1}{T_f} - \frac{1}{T_0}\right)\frac{\Delta H_{ice}}{R} \tag{13}$$

with T_0 the freezing point of pure water, ΔH_{ice} the latent heat of fusion for ice in (J/mol), R the universal gas constant. A convenient correlation between the mass fraction of ice y_{ice} and freezing point is the following (Van der Sman, 2008):

$$y_{ice} = y_{w0}\frac{T - T_f}{T - T_0} \tag{14}$$

with y_{w0} the initial moisture content of the food in the unfrozen state. Ignoring the difference in the mass density of liquid water and ice, we convert the mass fractions into volume fractions φ_i. For simplicity, we take the thermal material properties of salt equal to that of carbohydrates. As the amount of salt is minor, the introduced error is negligible.

The product of the effective mass density and effective specific heat is:

$$\rho_{eff} c_{p,eff} = \sum_i \varphi_i \rho_i c_{p,i} \tag{15}$$

and the effective thermal conductivity is modelled following Maxwell-Eucken (Van der Sman, 2008):

$$\lambda_{eff} = \lambda_c \frac{1 + (\varphi_{ice} + (1 - \varphi_{ice})Q)\Delta}{1 + (1 - \varphi_{ice})Q\Delta} \tag{16}$$

with $Q = \frac{1}{3}$. We neglect the tensorial character of the thermal conductivity induced by the dendritic growth of ice crystals along the direction of temperature gradient (van der Sman, 2021). λ_c is the thermal conductivity of the continuous, unfrozen phase, and $\Delta = (\lambda_{ice} - \lambda_c)/\lambda_c$, is the relative difference of thermal conductivities between the dispersed and continuous phase. For the continuous phase, we take the simple parallel model (Van der Sman, 2008):

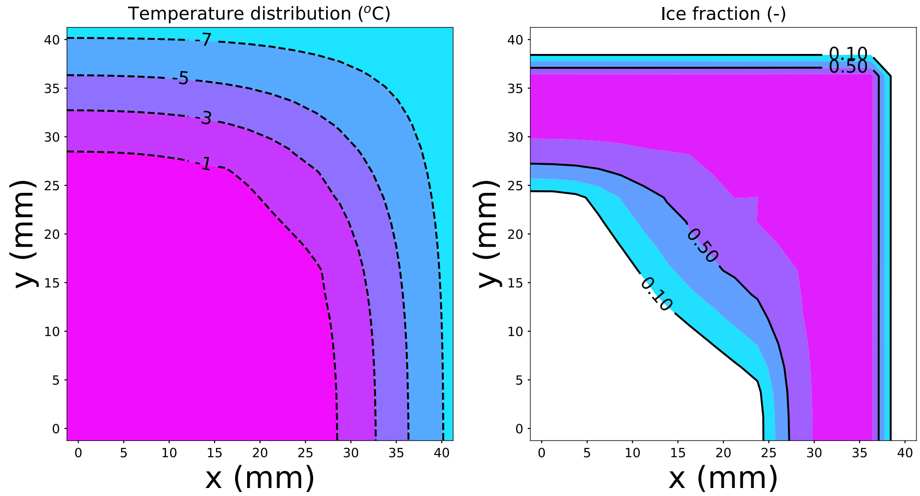

Fig. 2. Contour plots of the temperature and ice fraction distribution in the cross-section of a par-fried French fry after 5 min of freezing. The origin is at the center of the cross-section.

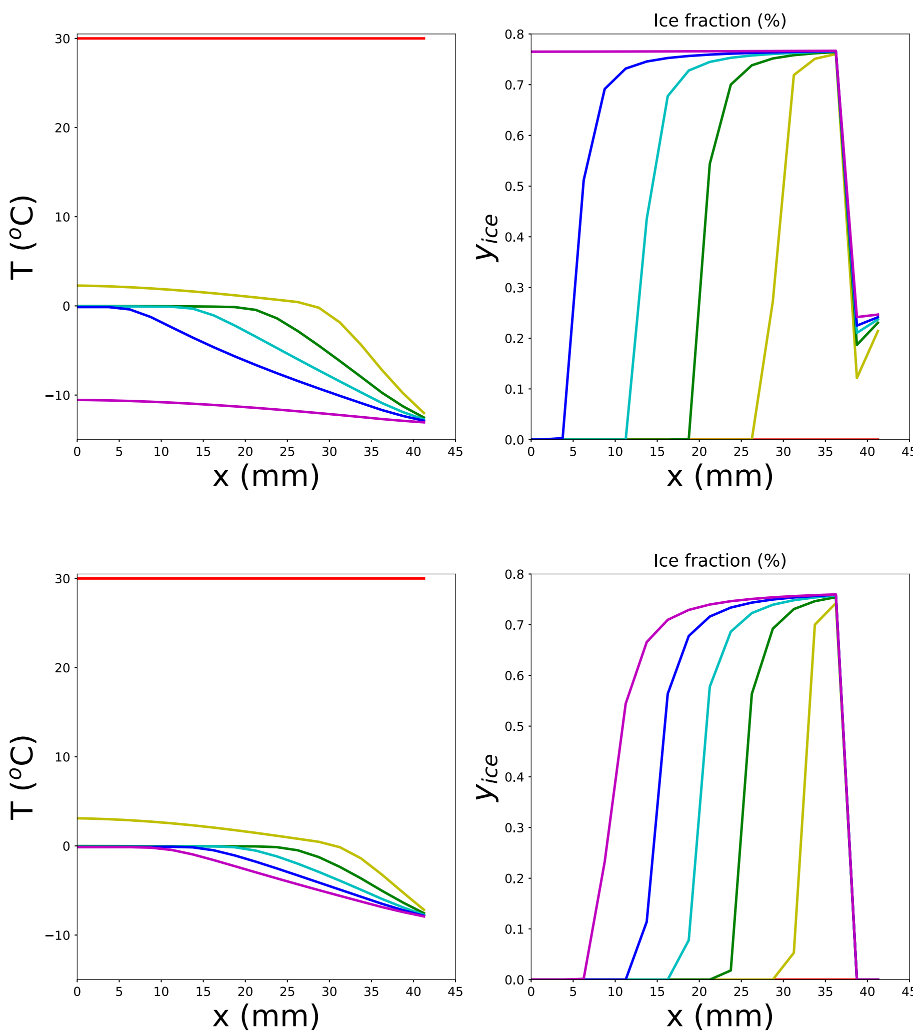

Fig. 3. Profiles of temperature and ice mass fraction y_{ice} as a function of distance, for the first 5 min of freezing, at 1-min intervals (red to magenta). The top pane shows simulations for $y_{w,crust} = 0.62$, and $T_{air} = -13^oC$, while the bottom pane shows results for $y_{w,crust} = 0.56$, and $T_{air} = -8^oC$. (For interpretation of the references to colour in this figure legend, the reader is referred to the Web version of this article.)

$$\lambda_c = \frac{\varphi_w \lambda_w + (\varphi_c + \varphi_s + \varphi_a)\lambda_s}{\varphi_w + \varphi_c + \varphi_s + \varphi_a} \quad (17)$$

with λ_i the thermal conductivity of component *i*. The values of λ_i are taken from (Van der Sman, 2008).

3. Experimental data

Parfrying experiments are performed with 9 mm thick strips. Before parfrying, the strips are blanched, such that starch is fully gelatinized. Next, they are soaked in a brine with salt and sugar. Subsequently, minimal drying is performed to remove surface water. Before parfrying, the potato strips had a moisture content of $y_w = 0.775$.

The par-frying is performed for a range of temperatures, $170 \leq T_{oil} \leq 190^oC$, and residence times, $40 \leq \tau_{fry} \leq 60$ s. Furthermore, slices 1 mm thick has been cut from the fry, which also contains part of the core. We have determined the water, oil, salt, and sugar content of these slices. We found that dry matter decreases linearly with the input of thermal energy: $Q \sim (T_{oil} - T_{boil})\tau_{fry} = E$. We assume that during par-frying the surface temperature quickly assumes the boiling temperature of $T_{boil} = 100^o$C. Before parfrying, the amount of salt and sugar is 3% and 0.5% of the total weight. In parfrying experiments, we varied the thermal energy input, such that $3000 \leq E \leq 6000$ K s, inducing a change in the water mass fraction of the sliced crust in the range $0.70 \leq y_{w,slice} \leq 0.67$. In our model, we will assume a crust region of thickness $\Lambda = 0.5$ mm. Hence, the mass fraction of water in the actual crust region ranges: $0.56 \leq y_{w,crust} \leq 0.62$.

Before entering the freezing tunnel, the fries are cooled down. The average temperature of fries entering the freezing tunnel is $T_{init} = 30^oC$. The freezing air temperature can range from $-14 \leq T_{air} \leq -8^oC$. For estimated airflow velocities (in the pore space between the fries) of about 2 m/s, we estimate a Nusselt number of $Nu = 40$, using the correlation for a packed bed of cylinders by (Zhukauskas, 1987). From the definition of $Nu = h_{ext}W/\lambda_{eff}$, we obtain a heat transfer coefficient of $h_{ext} \gg 1000$ W/m^2.K. Hence, we can assume that the outer surface takes the air temperature.

4. Results

Simulations are performed with $N = 18$. The crust region is assumed to be 0.5 mm, which is two lattice spacings thick. Via Eq. (7) the parameters Γ and ω are not uniquely defined. We have chosen for $\omega = 1.2$, and $Fo^* = 0.2$. During simulations, we have varied the freezing air temperature in the range $-14 \leq T_{air} \leq -8^oC$, and $0.56 \leq y_{w,crust} \leq 0.62$, with $y_{w,core} = 0.775$. Calculations show the initial freezing point of the core is $T_{f,core} = -0.135^oC$, while that of the crust ranges $-8.30 \leq T_{f,crust} \leq -7.87^oC$. Residence times of fries in the freezer tunnel are in the range $\tau_{freeze} = 11$–15 min.

In Fig. 2 we show a typical result of the simulation, showing contour plots of the temperature, and ice fraction after 5 min of freezing. Simulation is performed for $y_{w,crust} = 0.56$, $T_{air} = -8^oC$. Results show that the crust region is still unfrozen (with $\varphi_{ice} \approx 0$.

We compare the temperature profiles and ice fraction profiles along the horizontal axis for two extreme cases: a) $y_{w,crust} = 0.62$, and $T_{air} = -13^oC$, and b) $y_{w,crust} = 0.56$, and $T_{air} = -8^oC$. Fig. 3 shows the profiles for the first 5 min of freezing at a time interval of 1 min. We observe that for $T_{air} = -13^oC$ the fry is nearly fully frozen after 5 min, while for $T_{air} = -8^oC$ the ice front progresses somewhat slower (5 mm/min versus 7 mm/min), and the crust region is still unfrozen. At $T_{air} = -13^oC$ the crust region is fully frozen after 5 min, but the amount of ice is lower than the core region, because of its lower initial freezing point ($T_{f,crust} \approx -8^oC$). For both freezing conditions hold that after 11 min the cores are fully frozen. For $T_{air} = -8^oC$ the crust remains unfrozen, as its initial freezing point is near the freezing air temperature.

We note that in practice the French fries move as a packed bed with a height of 8–12 cm. Consequently, the freezing air will warm up, while flowing through the packed bed. Consequently, not all fries will experience an ambient temperature equal to the setpoint of T_{air}, which will also change with time. It is probable that in practice it takes 11–15 min to freeze all fries in the packed bed.

5. Conclusions

In this paper we have presented a 2D Lattice Boltzmann model for the problem of food freezing, using the particular example of par-fried french fries as an example. Next to its relevance of providing insight into this freezing problem related to practical quality problems of french fries, this Lattice Boltzmann model is of interest to food scientists because of the relative simplicity of the physics of the problem, as compared to the complex fluid flow problems (where the LB method has particular merits). Furthermore, it is showing an implementation of the enthalpy method for phase transition problems, which is rarely addressed in the LB community (Samanta et al., 2022).

For our case of freezing french fries, we have performed several simulations using fries with moisture already removed from the crust region, due to the action of parfrying. We have shown that for several practical processing conditions, the crust remains unfrozen, due to its lowered moisture content, and the amount of added sugars and salt. In other cases, the crust does get partially frozen, but much less than the core. These results are important inputs to the problem of crust fracturing during finish frying, as discussed in our companion paper (van der Sman and van den Oudenhoven, 2023).

Finally, we also like to note the similarity of parfrying before freezing, with dehydrofreezing (Agnelli et al., 2005; James et al., 2014; Schudel et al., 2021). In this process, foods are subject to a dehydration process, often via osmotic dehydration. The aim is to lower the initial freezing point and thus reduce the amount of ice and damage formed during freezing. The reduction of the amount of ice formed will also increase the freezing rate, and thus reduce ice crystal size (Van der Sman et al., 2013). After the dehydration step, one can still expect large gradients in moisture - leading to a strong variation of thermophysical properties. The presented Lattice Boltzmann model using the enthalpy method can also be used for freezing after dehydration. Due to the moisture gradients, one can also expect that some regions remain unfrozen. The actual modelling of the dehydration, combined with the volume shrinkage, is still a challenge for the Lattice Boltzmann method - where one commonly assumes a fixed grid. For 1-D problems, we have adapted the Lattice Boltzmann method for deforming grids (Van Der Sman, 2014), but this has to be generalized to higher dimensions still.

CRediT authorship contribution statement

R.G.M. van der Sman: I am the sole and corresponding author of the paper, I developed the concept, model, and wrote the full paper.

Declaration of competing interest

The authors declare that they have no known competing financial interests or personal relationships that could have appeared to influence the work reported in this paper.

Data availability

Data will be made available on request.

Acknowledgements

This research has been funded by 1) the Dutch Ministry of Economic Affairs under contract LWV21.73, project Integral sustainability improvement of the frozen vegetables and potato processing chains, and 2) Lamb-Weston Meijer.

References

Agnelli, M., Marani, C., Mascheroni, R., 2005. Modelling of heat and mass transfer during (osmo) dehydrofreezing of fruits. J. Food Eng. 69, 415–424.

Chen, S., Doolen, G.D., 1998. Lattice Boltzmann method for fluid flows. Annu. Rev. Fluid Mech. 30, 329–364.

Fadiji, T., Ashtiani, S.H.M., Onwude, D.I., Li, Z., Opara, U.L., 2021. Finite element method for freezing and thawing industrial food processes. Foods 10, 869.

Farid, M., 2002. The moving boundary problems from melting and freezing to drying and frying of food. Chem. Eng. Process: Process Intensif. 41, 1–10.

Huang, R., Wu, H., Cheng, P., 2013. A new lattice Boltzmann model for solid–liquid phase change. Int. J. Heat Mass Tran. 59, 295–301.

Huo, Y., Rao, Z., 2017. The quasi-enthalpy based lattice Boltzmann model for solid-liquid phase change. Appl. Therm. Eng. 115, 1237–1244.

James, C., Purnell, G., James, S.J., 2014. A critical review of dehydrofreezing of fruits and vegetables. Food Bioprocess Technol. 7, 1219–1234.

Kiani, H., Zhang, Z., Sun, D.W., 2015. Experimental analysis and modeling of ultrasound assisted freezing of potato spheres. Ultrason. Sonochem. 26, 321–331.

Kromkamp, J., van den Ende, D., Kandhai, D., van der Sman, R., Boom, R., 2006. Lattice Boltzmann simulation of 2d and 3d non-brownian suspensions in Couette flow. Chem. Eng. Sci. 61, 858–873.

LeBlanc, D.I., Kok, R., Timbers, G.E., 1990. Freezing of a parallelepiped food product. part 2. comparison of experimental and calculated results. Int. J. Refrig. 13, 379–392.

Mannapperuma, J., Singh, R., 1988. Prediction of freezing and thawing times of foods using a numerical method based on enthalpy formulation. J. Food Sci. 53, 626–630.

Samanta, R., Chattopadhyay, H., Guha, C., 2022. A review on the application of lattice Boltzmann method for melting and solidification problems. Comput. Mater. Sci. 206, 111288.

Scheerlinck, N., Verboven, P., Fikiin, K., De Baerdemaeker, J., Nicolaï, B., 2001. Finite element computation of unsteady phase change heat transfer during freezing or thawing of food using a combined enthalpy and Kirchhoff transform method. Transact. ASAE 44, 429.

Schudel, S., Prawiranto, K., Defraeye, T., 2021. Comparison of freezing and convective dehydrofreezing of vegetables for reducing cell damage. J. Food Eng. 293, 110376.

Van der Graaf, S., Nisisako, T., Schroën, C., Van Der Sman, R., Boom, R., 2006. Lattice Boltzmann simulations of droplet formation in a t-shaped microchannel. Langmuir 22, 4144–4152.

Van der Sman, R., 1997. Lattice-Boltzmann scheme for natural convection in porous media. Int. J. Mod. Phys. C 8, 879–888.

Van der Sman, R., 2006. Finite Boltzmann schemes. Comput. Fluid 35, 849–854.

Van Der Sman, R., 2006. Galilean invariant lattice Boltzmann scheme for natural convection on square and rectangular lattices. Phys. Rev. 74, 026705.

Van der Sman, R., 2008. Prediction of enthalpy and thermal conductivity of frozen meat and fish products from composition data. J. Food Eng. 84, 400–412.

Van der Sman, R., 2012. Thermodynamics of meat proteins. Food Hydrocolloids 27, 529–535.

Van Der Sman, R., 2014. Moisture transport in swelling media modelled with a lattice Boltzmann scheme having a deforming lattice. J. Food Eng. 124, 54–63.

Van der Sman, R., 2018. Clumping of frozen par-fried foods: lessons from frosting on structured surfaces. Food Struct. 17, 9–20.

van der Sman, R., 2021. Multiscale simulations of directional ice crystal growth in sugar solutions. Food Struct. 30, 100214.

Van der Sman, R., Broeze, J., 2014. Effects of salt on the expansion of starchy snacks: a multiscale analysis. Food Funct. 5, 3076–3082.

Van der Sman, R., Ernst, M., 1999. Diffusion lattice Boltzmann scheme on a orthorhombic lattice. J. Stat. Phys. 94, 203–217.

Van der Sman, R., Meinders, M., 2011. Prediction of the state diagram of starch water mixtures using the flory–huggins free volume theory. Soft Matter 7, 429–442.

van der Sman, R., van den Oudenhoven, B., 2023. Dust formation in French fries. Curr. Res. Food Sci. 6, 100466.

van der Sman, R.G., Van der Graaf, S., 2008. Emulsion droplet deformation and breakup with lattice Boltzmann model. Comput. Phys. Commun. 178, 492–504.

Van der Sman, R., Voda, A., Van Dalen, G., Duijster, A., 2013. Ice crystal interspacing in frozen foods. J. Food Eng. 116, 622–626.

Wang, H., Yuan, X., Liang, H., Chai, Z., Shi, B., 2019. A brief review of the phase-field-based lattice Boltzmann method for multiphase flows. Capillarity 2, 33–52.

Zhao, Y., Takhar, P.S., 2017. Freezing of foods: mathematical and experimental aspects. Food Eng. Rev. 9, 1–12.

Zhukauskas, A., 1987. Convective heat transfer in external flows. J. Eng. Phys. 53, 1240–1246.